

Simultaneous Energy Harvesting and Gait Recognition using Piezoelectric Energy Harvester

Dong Ma, *Student Member, IEEE*, Guohao Lan, *Member, IEEE*, Weitao Xu, *Member, IEEE*,

Mahbub Hassan, *Senior Member, IEEE*, and Wen Hu, *Senior Member, IEEE*,



Abstract—Piezoelectric energy harvester, which generates electricity from stress or vibrations, is gaining increasing attention as a viable solution to extend battery life in wearables. Recent research further reveals that, besides generating energy, PEH can also serve as a passive sensor to detect human gait power-efficiently because its stress or vibration patterns are significantly influenced by the gait. However, as PEHs are not designed for precise measurement of motion, achievable gait recognition accuracy remains low with conventional classification algorithms. The accuracy deteriorates further when the generated electricity is stored simultaneously. To classify gait reliably while simultaneously storing generated energy, we make two distinct contributions. First, we propose a preprocessing algorithm to filter out the effect of energy storage on PEH electricity signal. Second, we propose a long short-term memory (LSTM) network based classifier to accurately capture temporal information in gait-induced electricity generation. We prototype the proposed gait recognition architecture in the form factor of an insole and evaluate its gait recognition as well as energy harvesting performance with 20 subjects. Our results show that the proposed architecture detects human gait with 12% higher recall and harvests up to 127% more energy while consuming 38% less power compared to the state-of-the-art.

Index Terms—Piezoelectric Energy Harvesting, Simultaneous Energy Harvesting and Sensing, Gait Recognition, Deep Learning, LSTM

1 INTRODUCTION

Piezoelectric energy harvester (PEH), which can harvest electrical energy from mechanical stress or vibration, has become an attractive solution to power many industrial sensor nodes [1], [2], as well as wearable devices [3], [4], [5]. Interestingly, because PEH energy harvesting is influenced

by the surrounding contexts, the same PEH can also serve as an energy-free sensor to detect a wide range of machine and human contexts, such as measuring the airflow of air conditioning systems [6], detecting human activities [7], demodulating acoustic communications [8], and many more as surveyed in [9].

Given that gait recognition is considered as an attractive option for human identification and authentication [10], our focus in this paper is to explore reliable gait recognition in wearable devices using PEH as a passive sensor. A recent attempt by Xu et al. [11] revealed that although PEH can detect gait 82% more power-efficiently than conventional sensors, i.e., accelerometers, it cannot match the high recognition accuracy achievable with accelerometers. A further limitation of the work in [11] is that the authors used the PEH only as a sensor, but the generated electricity was not harvested in a capacitor. Thus the interference caused by energy harvesting on the PEH-generated AC voltage and its resulting impact on gait recognition performance was not captured by the experiments in [11]. As a matter of fact, the impact of energy harvesting on the sensing performance of PEH was found to be significant, e.g., in airflow monitoring study [6], which forced existing solutions to employ separate PEHs, i.e., one dedicated to sensing only, while the other is used for energy harvesting. As dedicated use of PEH increases hardware cost and complexity, we seek solutions that can realize simultaneous energy harvesting as well as reliable gait recognition using the same piece of PEH. Finally, the work in [11] considered gait recognition from PEH embedded in hand-held devices, which generated extremely small amount of power as walking-induced PEH vibrations have low energy density. Our goal is to design a PEH-based gait recognition system that can detect gaits reliably while generating sufficient energy that can be of practical use.

The major contributions of this work are summarized as follows:

- We design a novel simultaneous energy harvesting and gait recognition architecture, called simultaneous energy harvesting and sensing (SEHS). In this architecture, we propose a classifier based on long short-term memory (LSTM) deep neural network to accurately

Dong Ma is with the School of Computer Science and Engineering, University of New South Wales (UNSW), Sydney, Australia, and also with the Data61, CSIRO, Eveleigh, Australia (E-mail: dong.ma1@unsw.edu.au).

Guohao Lan is with the Department of Electrical and Computer Engineering, Duke University, Durham, NC 27708, USA (E-mail: guohao.lan@duke.edu). The work was done when the author was with UNSW.

Weitao Xu is with the Department of Computer Science, City University of Hong Kong, Hong Kong (e-mail: weitaoxu@cityu.edu.hk). The work was done when the author was with UNSW.

Mahbub Hassan is with the School of Computer Science and Engineering, University of New South Wales (UNSW), Sydney, Australia (E-mail: mahbub.hassan@unsw.edu.au).

Wen Hu is with the School of Computer Science and Engineering, University of New South Wales (UNSW), Sydney, Australia (E-mail: wen.hu@unsw.edu.au).

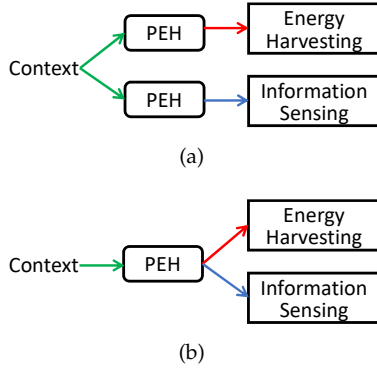


Fig. 1: (a) Requirement of separate PEHs for energy harvesting and sensing in existing architecture [6], and (b) use of the same PEH for simultaneous energy harvesting and sensing in the proposed SEHS architecture.

capture the temporal information latent in gait-induced electricity generation. We further devise a preprocessing algorithm to filter out the effect of energy storage on the PEH electricity signal as much as possible before the signal is fed to the classifier.

- We implement the proposed SEHS architecture using off-the-shelf PEH inside a shoe sole, which allows a large amount of energy generation from direct foot strikes during walking.
- We evaluate the performance of the implemented SEHS prototype with 20 subjects. We observe that the proposed LSTM can learn the gait patterns directly from the raw signals without filtering or preprocessing, whereas, existing classifiers struggle without filtering. With the proposed filtering, our results show that SEHS can detect human gait with 12% higher recall and harvests up to 127% more energy while consuming 38% less power compared to the state-of-the-art presented in [11].

The rest of the paper is organized as follows. Section 2 illustrates the effect of PEH energy harvesting on its sensing signal and presents the proposed filtering algorithm to minimize this effect. Design of LSTM neural networks for gait classification is presented in Section 3. Section 4 presents SEHS prototyping and its evaluation in terms of both gait recognition and energy harvesting performance. Current limitations and potential solutions are discussed in Section 5, followed by a review of related works in Section 6. We conclude the paper in Section 7.

2 SEHS DESIGN

In this section, we present the design of the proposed SEHS architecture, illustrate the effect of energy harvesting on the sensing signal, and explain the proposed filtering algorithm to minimize the effect of energy harvesting on information sensing.

2.1 Limitations of Current Architecture

Most prior works on PEH-based sensing [11], [12], [13] only considered the sensing circuit without implementing energy harvesting and storage components, i.e., no capacitor

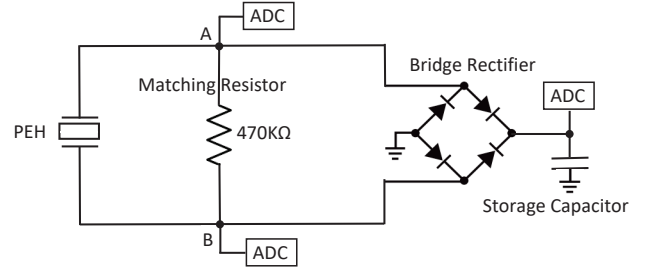


Fig. 2: Circuit design of the proposed SEHS architecture.

was included in the circuit to store the harvested energy, where the main focus is to demonstrate various sensing capabilities of PEH. In [6], Xiang et al. built a self-powered airflow monitoring system in which one PEH was utilized to sense the speed of airflow and the other to harvest energy from vibrations caused by the airflow. By using two PEHs, this approach completely avoids any interference from the interactions between harvesting and sensing. However, it increases system complexity, form factor, and cost.

2.2 Design of the Proposed SEHS

As shown in Figure 1, the aims of the SEHS design are to (1) store the harvested energy, i.e., the rectified AC voltage generated by the PEH, in a capacitor, and (2) read the same AC voltage for context sensing using minimal power consumption. Unfortunately, reading the PEH AC voltage requires some additional processing, which would consume some power. Note that PEH generates electric potential proportional to the applied strain [14] and the polarization of the generated electricity corresponds to the direction of the induced deformation, producing the alternating voltage (AC). PEH usually generates an open-circuit AC voltage within minus decades volts to decades volts [15], while the commonly used ADC (Analog-to-Digital Converter) can only measure the non-negative voltage ranging from 0V to 5V. Consequently, the voltage signal cannot be acquired when PEH output is directly connected to ADC. To address this problem, most existing works utilize an amplifier [6] or voltage divide circuit [13], [16] to measure the AC voltage using a single ADC channel, which consumes several hundreds of μW .

One of our design goals is to minimize the sensing related power consumption. We achieve this by trading off voltage divider with additional ADC channels, as ADC channels consume very little power on the order of 1-2 μW . Figure 2 shows the circuit design of the proposed SEHS architecture. A matching resistor is used to limit the peak amplitude of the AC voltage within the ADC readable range. Instead of using a single ADC channel to capture the whole AC waveform, we use two ADC channels, i.e., point A (V_A) and point B (V_B), to measure the voltage on the matching resistor. Since the two points are directly connected to the output of PEH, the generated voltage, V , can be easily derived by subtracting the measured voltage at point B from point A (both are non-negative values), i.e., $V = V_A - V_B$. The energy flows to the capacitor through a full-bridge rectifier which is used to convert the

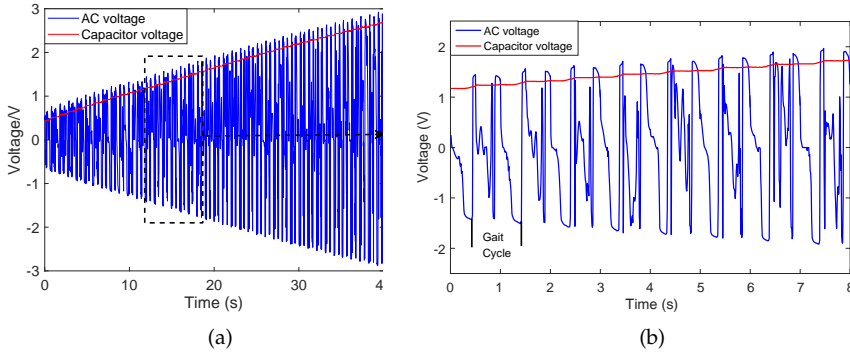


Fig. 3: (a) The original AC voltage and capacitor voltage and (b) its magnified version for a short period.

AC voltage to DC voltage. With this circuit, the proposed SEHS architecture is able to collect the voltage signal and store the generated energy by using the same piece of PEH hardware.

2.3 Effect of Energy Storage on Sensing

Unfortunately, when a capacitor is used to store the harvested energy, its dynamic states (stored energy) modifies the current or AC voltage signal generated by the PEH. To illustrate the effect of energy harvesting on AC voltage reading, we collected data when our circuit was used in the shoe of a waking subject (see Section 4.1 for prototype details). Figure 3 illustrates the waveform of the sampled AC voltage signal as well as the capacitor voltage. Intuitively, the peak-to-peak amplitude of the AC voltage should be approximately identical, as the entire trace is extracted from the same person while walking with a consistent style [11]. However, we can see that the peak-to-peak amplitude of the AC voltage is actually increasing with time as the capacitor voltage rises, i.e., more energy is being stored. The similar phenomenon is also described in [6].

The observed effect of energy harvesting on AC voltage in Figure 3 can be explained as follows. Using capacitor theory [17], Figure 4 illustrates how the charging current decreases while the capacitor is being charged. This theory reveals that the current flow to the PEH is dropping when energy is being harvested and stored in the capacitor. Note that the PEH has a large internal resistance on the order of $M\Omega$ [6], [18] and the output voltage is determined by the load resistance as well as the internal resistance [18], [19]. With the current flow decreased, the voltage on the internal resistance of PEH is reduced. As a result, the amplitude of the output voltage is increased, which explains the increasing peak-to-peak amplitude of the AC voltage in Figure 3.

How to minimize the distortion of the sensing signal in a SEHS architecture remains an open problem. Note that the state-of-the-art in [6] did not actually solve this problem, but instead used two separate PEHs to avoid this issue. In the following subsection, we propose a filtering algorithm that can minimize the distortion effect of energy harvesting on the sensing signal.

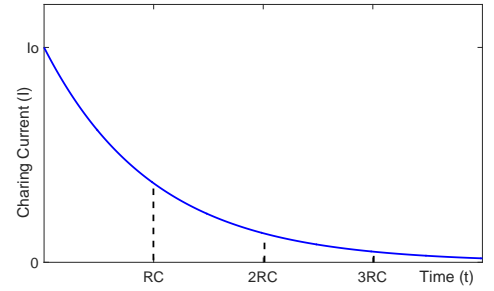


Fig. 4: Capacitor charging current as a function of time. RC is the time constant and I_0 is the initial current when capacitor voltage is 0.

2.4 Filtering Algorithm

From Figure 3, we can observe that the main effect of storing energy is on the amplitude of AC voltage, where the amplitude continues to increase with increasing capacitor voltage. The aim of the filtering algorithm, therefore, is to prevent the increasing capacitor voltage from lifting the AC voltage without destroying the pattern of the signal. Algorithm 1 shows the proposed filtering algorithm, where $V_A(t)$ and $V_B(t)$ represent the voltage at time t measured at point A and B, respectively, as shown in Figure 2 with $V'_A(t)$ and $V'_B(t)$ representing their corresponding filtered values. At time t , $V_C(t)$ is the capacitor voltage and $V'(t)$ is the final AC voltage used for gait recognition. We introduce a constant, V^* , to compensate the impact of capacitor voltage. Particularly, when $V_A(t)$ (or $V_B(t)$) is higher than $V_C(t)$, the capacitor is being charged and its current voltage directly lifts the actual voltage at point A (or B). Thus, we obtain the difference between $V_A(t)$ and $V_C(t)$ and add it to V^* (line 4). When $V_A(t)$ (or $V_B(t)$) is lower than $V_C(t)$, we multiply V^* by the proportion of $V_A(t)$ and $V_C(t)$ to retain the gait patterns (line 6). Since the amplitude of the filtered signal is affected by the choice of V^* , we will evaluate the impact of V^* on recognition performance in Section 4.4.2.

The complexity of the filter is $O(N)$ (N is the number of samples), which suggests that it can be implemented with-

Algorithm 1: Proposed Filtering Algorithm

Input: $V_A(t), V_B(t), V_C(t), V^*$

Output: $V'_A(t), V'_B(t), V'(t)$

1 **Main procedure:**

2 **for** $t = 1, 2, \dots, N$ **do**

3 **if** $V_A(t) \geq V_C(t)$ **then**

4 $V'_A(t) = V_A(t) - V_C(t) + V^*$;

5 **else**

6 $V'_A(t) = V^* * (V_A(t)/V_C(t))$;

7 **end**

8 **the same operation for** $V_B(t)$;

9 **obtain** $V'_B(t)$;

10 $V'(t) = V'_A(t) - V'_B(t)$;

11 **end**

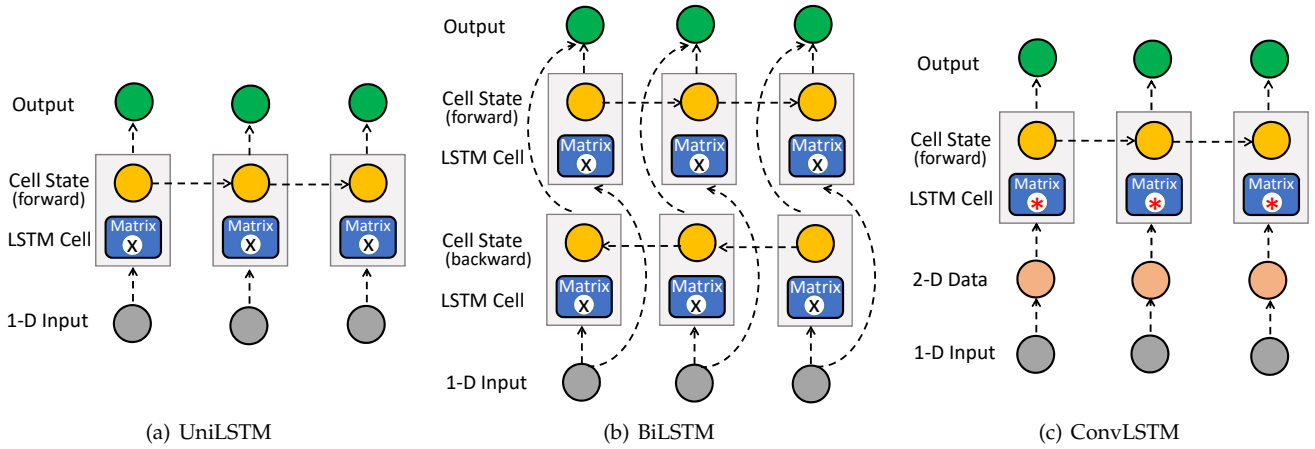


Fig. 5: Network structure comparison of three LSTM variants: (a) UniLSTM, (b) BiLSTM, and (c) ConvLSTM. The symbol \times and $*$ represent multiplication and convolution operation, respectively.

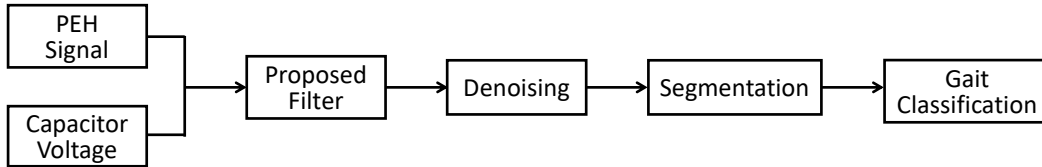


Fig. 6: System model of gait recognition using SEHS.

out significant computational burden. Note that the filter requires the capacitor voltage (V_C) as input, which can be easily obtained using an additional ADC channel as shown in our circuit design (Figure 2). Use of additional ADC channels contributes minimal power consumption overhead as will be demonstrated in our measurements in Section 4.6.

3 LSTM-BASED GAIT CLASSIFICATION

A gait cycle is basically sequential movements of human body that usually involve six main phases: heel strike, foot flat, mid-stance, heel-off, toe-off, and mid-swing [20]. These phases are interrelated and the characteristics of former phases interfere with the later ones (i.e., there exists temporal correlation), thereby forming a unique gait pattern of each individual. Thus, we propose to use the long short-term memory (LSTM) neural networks [21] for gait classification due to its superior performance on learning information from sequences/signals with high temporal correlation [22], [23], [24]. LSTM neural networks exhibit a chain-like structure consisting of multiple cells, where the input of each cell is a sample in a time series data. The core idea behind LSTMs is the cell state which looks like a conveyor belt and preserves the memory of the network [25]. By dynamically updating the cell state, previous information that is useful to current state can be retained.

In this work, we consider three variants of LSTM, i.e., unidirectional LSTM (UniLSTM), bidirectional LSTM (BiLSTM) [26], and convolutional LSTM (ConvLSTM) [27], as compared in Figure 5. UniLSTM processes sequential data in forward direction thus only preserving information of the past. In contrast, BiLSTM has two cell states which can preserve information of both the past and future by running

in forward and backward direction, respectively. In general, BiLSTM has better performance than UniLSTM as temporal correlations from both directions can be learned. ConvLSTM is just like UniLSTM, but internal matrix multiplications are exchanged with convolution operations. It is usually used in sequential image data (e.g., video) processing so that the one-dimensional PEH data should be converted to two-dimensional data before feeding to the LSTM cells.

The three models are designed as follows. Each LSTM variant has one LSTM layer containing N cells, where N is the number of samples in a gait cycle. Each cell is composed of 32 hidden units (the choice of 32 was arrived empirically to prevent over-fitting while keeping good recognition accuracy). On top of that, a fully connected layer is used to convert the output matrix of the LSTM network into a class vector, i.e., the probability of current instance to each class. Then, we apply a *softmax* layer to obtain the final class by selecting the class with maximum probability.

4 EVALUATION

The system model for evaluating gait recognition using SEHS is illustrated in Figure 6. Specifically, we first built an insole-based prototype to collect data from subjects. Then, the proposed filter is applied to the collected PEH signal and capacitor voltage to minimize the interference of energy storage. Afterwards, the filtered signal is denoised and segmented before feeding to the LSTM-based classifiers. With the framework, we then evaluate the performance of gait recognition and energy harvesting. Finally, as the filter requires the capacitor voltage as input, we explore its practicability by measuring the power overhead of sampling the capacitor voltage.

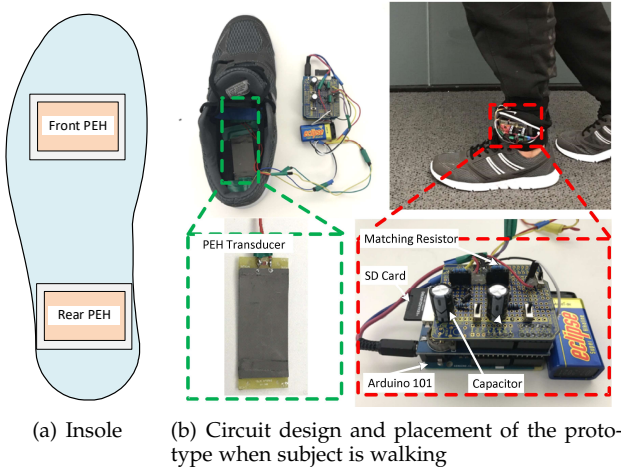


Fig. 7: The design and appearance of the SEHS prototype.

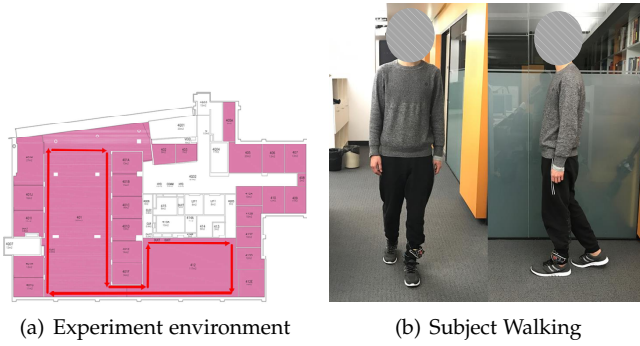


Fig. 8: Data collection setup.

4.1 SEHS Prototyping

Figure 7 shows the prototype we designed and implemented in the form factor of a shoe to harvest energy during human walking and detect the user gait at the same time using the PEH voltage signal. The prototype includes two PEHs from Piezo System [28] mounted on the front and rear of the insole (refers to PEHFront and PEHRear), which are used to investigate the impact of PEH placement on the gait recognition accuracy. AC voltages from the PEHs are rectified by a full-bridge diodes rectifier and charged into two $1000\mu F$ electrolytic capacitors. The output voltage and capacitor voltage are sampled by an Arduino 101 [29] board, which is equipped with an Intel Curie microcontroller. A sampling rate of 100 Hz is used for data collection and the sampled data is saved on a 4GB microSD connected to the Arduino using a microSD shield. A nine volts battery powers the whole system. To help users collect data, the prototype contains three switches, one is to control the start and stop of data collection and the other two for controlling the charging and discharging of the two capacitors respectively. The entire Arduino board is placed outside the shoe.

The Arduino 101 measures voltage between 0 and 5 volts and provides 10 bits of resolution, i.e., 1024 different values. The corresponding output voltages from the measurements,

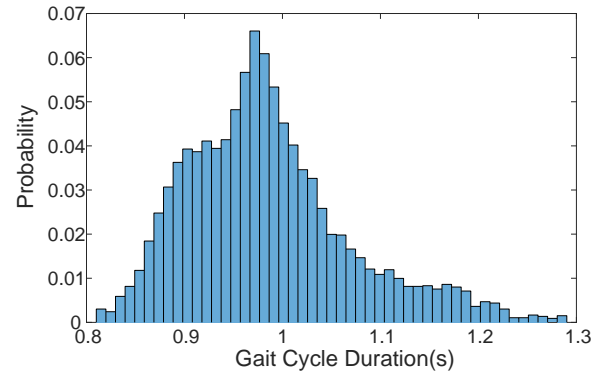


Fig. 9: Distribution of gait cycle duration.

therefore, are obtained as:

$$voltage = \frac{5 * ADC \text{ measurement}}{1024} \quad (1)$$

4.2 Data Collection and Pre-processing

During the data acquisition stage, we create the dataset by asking 20 healthy volunteers, including 16 males and 4 females¹, to walk along the specified route as shown in Figure 8(a). Each volunteer is asked to wear a shoe equipped with the designed insole in their left foot and the data collection module is attached to the ankle position as shown in Figure 8(b). The participants are suggested to walk in his/her normal walking style and speed. The data collection duration is approximately 300 seconds and the subjects need to toggle the switch to discharge the capacitors every 50 seconds. The reason is that the accumulated voltage on the capacitor will exceed 5V when walking for a certain period of time (around 55 seconds in our tests), so that it can not be measured. More importantly, high voltage may damage the ADC module of the board.

We collect a time series of voltage signal of the PEHs when subjects are walking, in which the signal follows a cyclic pattern reflecting the gait of each subject. As shown in Figure 3(b), there are two peaks within one gait cycle, which indicate the heel strike and toe-off time of the foot respectively. Firstly, the moving average function and a low pass filter with the cutoff frequency of 10 Hz are used to eliminate out-band interference. We then apply a bandpass filter to detect these peaks and the gait cycle is obtained by combining the samples between two consecutive peaks together. Since the walking pattern varies from different subjects, we tune the lower and upper cutoff frequency of the bandpass filter for each subject ranging from 0.5Hz to 3Hz to enable an accurate gait cycle segmentation.

After the peak detection and samples combination, gait cycles with different time duration are available. Figure 9 plots the distribution of the gait cycle duration of the 20 subjects who are suggested to walk in their normal speed. It is clear that the time duration of one gait cycle varies from 0.8s to 1.3s. To deal with such variable walking speeds that

1. Ethical approval for carrying out this experiment has been granted by the corresponding organization (Approval Number HC15888).

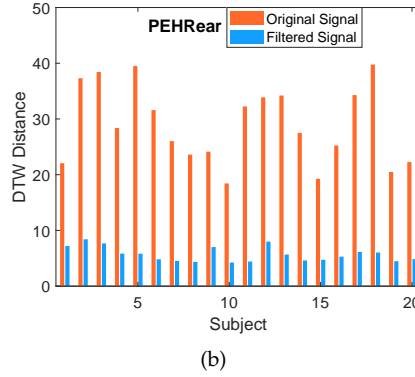
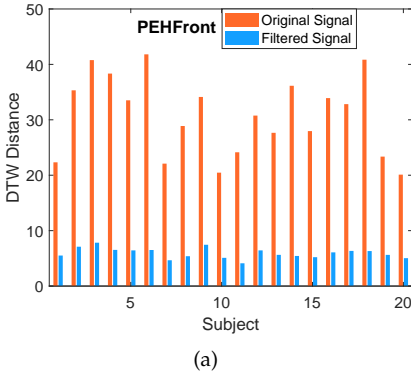


Fig. 10: Similarities among individual gaits of the same subject for original vs. filtered signals: (a) front PEH and (b) rear PEH. Lower DTW distance means higher similarity.

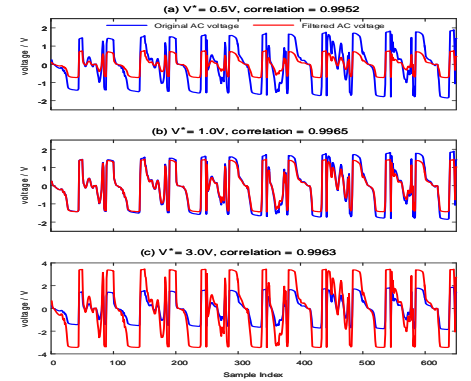


Fig. 11: Waveform comparison for AC voltage with and without filtering.

may occur among different subjects or one subject in different walking scenarios, we perform the linear interpolation on the detected gait cycles. According to the distribution of the gait cycle length, the number of samples in one gait cycle ranges from 80 to 130 with the sampling rate of 100 Hz. Thus, we interpolate the gait cycles to equal length with 130 samples.

Accurate gait pattern extraction is a critical factor that affects gait recognition accuracy. In our experiment, volunteers were asked to walk in a square environment as shown in Figure 8(a) for several minutes, during which they experienced several turnings and some short pauses. Obviously, the detected gait cycles within these periods contain distorted gait patterns. Therefore, it is important to omit these unusual cycles to keep high recognition accuracy. We employ Dynamic Time Warping (DTW) to delete unusual cycles for each subject. In detail, the average distance of all the gait cycles are computed firstly and treated as the typical cycle. Then, the distance between each cycle and the typical cycle is calculated. We detect and omit the irregular cycles by a simple threshold method, i.e. if the DTW distance of a detected cycle is higher than a predefined value, it will be dropped. The DTW distance reflects the similarity among a given cycle and the rest cycles of the subject. We collect around 280 to 300 gait cycles for each subject. To achieve a fair classification, we extract 250 gait cycles per subject after performing irregular cycle deletion. In total, a $2 \times 20 \times 250$ gait cycle dataset is created and utilized to evaluate the performance of the proposed SEHS architecture and filter.

4.3 Training and Classification

Then, we use the three designed LSTM networks for gait classification. We split the collected dataset into the training set (80%) and testing set (20%), and train the models with 5-fold cross validation mechanism. During training, the loss function and optimizer are set to cross-entropy and Adam, respectively. In addition, we set batch size to 64 and utilize the *EarlyStopping* [30] mechanism to prevent model overfitting. After training, the testing set is delivered to the trained models and the classification results are obtained for accuracy calculation. All the procedures are implemented with Keras in Python running on Tensorflow 2.0 platform.

In addition, we consider three benchmark classifiers: Support Vector Machine (SVM), K-Nearest Neighbor (KNN), and Sparse Representation based Classification (SRC) [31]. SVM and KNN are two typical machine learning based classifiers adopted in a multitude of sensing applications like human activity recognition. We extract 22 statistical features [32] from both time and frequency domain for each gait cycle and use them as the input to the two classifiers. SRC automatically mines features using sparse representation and has been proved to be more robust to environmental noise in sensing tasks. Moreover, it was applied to the state-of-the-art [11] that uses PEH for gait recognition. Like LSTM, SRC can be regarded as a featureless classifier so that we feed complete gait cycles to it during classification. We perform 5-fold cross-validation on the collected dataset and all the classifications for the three benchmarks are carried out in MATLAB.

4.4 Performance Evaluation

Next, we evaluate the performance of the proposed SEHS architecture, filter, and LSTM neural networks based on the collected dataset in the following aspects. Firstly, we use DTW distance [33] and Pearson correlation [34] to explore the effectiveness of the proposed filtering algorithm from the signal waveform aspect. Secondly, we evaluate the filter from the perspective of gait recognition performance (e.g., precision and recall), under different system parameters, such as sampling rate and classifier.

4.4.1 Filter Performance

Since gait cycles of the same person are expected to be similar during a normal walk, such *gait similarity* can be used to assess the performance of the proposed filter algorithm. Due to the distortion effect of energy harvesting, we can expect that the gait similarity among different cycles for the original AC signal would be low, but would increase when the filter is applied. For each subject and each PEH, we computed gait similarity for a given trace of 250 gait cycles as the average DTW (dynamic time warping) distance between all possible pairs of gait cycles. The lower the DTW distance, the higher the gait similarity for samples from each subject. Figures 10(a) and 10(b) compare DTW distance

of signals from the two PEHs for each of the 20 subjects. We can clearly see that the gait similarities for the filtered signal are consistently higher (or the DTW distance is $5\times$ lower) than those for the original signal, irrespective of the subjects and position of PEH. This provides evidence that the proposed filtering algorithm has successfully reduced signal distortions caused by energy harvesting.

Figure 11 compares the waveform of the original AC voltage (blue) and the filtered version (red) for different values of V^* . Visually, we can see that irrespective of the value chosen for V^* , the filtered signal matches well with the original signal. In addition, we calculate the Pearson correlation coefficient between the original signal and filtered signal. The Pearson correlation coefficient ranges between -1 and 1 , where 1 means total positive linear correlation, 0 means no linear correlation, and -1 means total negative linear correlation. For different V^* , the calculated correlation coefficients are all around 0.996 , suggesting that our filter successfully retains the gait pattern of the original signal. Next, we investigate whether the value of V^* will affect the gait recognition performance.

4.4.2 Gait Recognition Performance

Impact of V^* : To do that, we applied the proposed filter with different value of V^* (from $0.5V$ to $4V$) on the original signal and calculate the recognition recall of the filtered signals. All the three LSTM variants are considered and the PEHFront and PEHRear are evaluated separately. As shown in Figure 12, all the curves are almost flat, indicating that recognition recall is not affected by the chosen of V^* . So, we select a typical value of $2V$ for the rest of evaluation.

Gait Recognition Recall vs. Sampling Rates: Given that walking is a low-frequency activity, a sampling rate of 100 Hz might be excessive for capturing the latent gait patterns. We downsample each gait cycle to investigate the minimal sampling rate required, which would result in less sensing and computation power consumption. For different sampling rates, Figure 13 compares the gait recognition recall obtained with and without filtering for both PEHs using the three LSTM-based classifiers. It is clear that for all sampling rates, filtered signal outperforms the original counterpart. In addition, the recognition recall starts to saturate when sampling rate is higher than 40 Hz, which suggests that such sampling rate is sufficient to capture the gait patterns. We will therefore consider a sampling rate of 40 Hz in the subsequent analysis.

Gait Recognition Recall vs. Classifiers: Then, we evaluate the gait recognition performance of the filter against different classifiers. The parameters in SVM and KNN are tuned to provide the highest accuracy. For SVM classifier, we choose quadratic kernel and the box constraint level is set to 5 . For KNN classifier, the number of nearest neighbours is set to 10 . For each classifier, we train five different models while do inference with a fixed testing dataset. The average recognition accuracy (precision and recall) and corresponding standard deviation are presented.

Table 1 compares the gait recognition performance of the proposed three LSTM variants and three benchmark classifiers. We can clearly see that the filtered signals outperform the original counterparts for all the six classifiers in terms

of recognition precision and recall. Our filter improves the recognition recall by 8% - 10% for machine learning based classifiers and 2% - 7% for LSTM based classifiers, which provides strong evidence that the proposed filter is robust and effective across the choice of classifiers. This result also reveals that LSTMs show better performance in learning from noisy PEH data, while conventional machine learning methods struggle without filtering.

For the three LSTM variants, BiLSTM achieves the best performance due to its capability to learn temporal correlation from both the forward and backward direction. Compared to UniLSTM, ConvLSTM achieves even lower accuracy which might because the temporal correlation is deteriorated when converting the 1-D sequential signal into 2-D data. In addition, compared to previous work [11] using SRC for PEH-based gait recognition, the proposed BiLSTM classifier significantly improves the recognition recall by up to 12% . Another interesting finding is that the front PEH and rear PEH achieve almost identical accuracy (within error margin), which suggests that both PEH are capable of capturing gait information of the wearer.

Gait Recognition Recall vs. Training Sample Size: In the above analysis, we perform 5-fold cross-validation on the collected dataset, i.e., 200 gait cycles from each subject are used to train the model. On one hand, collecting massive amount of data increases the burden on users. On the other hand, given that deep learning usually requires abundant training data, it is unsure whether the collected dataset is large enough to fully learn the latent gait patterns. So, with filtered data from both PEHs, we fix the testing dataset and reduce the number of training sample to investigate how the recognition recall changes. The experiment is run with BiLSTM due to its superior performance. As shown in Figure 14, the recognition recall grows sharply with the increasing training size when the number of training sample is small, while it starts to saturate when each subject provides 150 samples. This reveals that the collected dataset is enough for the proposed shallow deep neural networks (one layer). We also observe that with 50 training samples per user, a recognition recall of 96% is obtained, which achieves a balance between user burden and recognition performance.

4.5 Analysis of Harvested Energy

In SEHS, not only the voltage signal is collected, but also the generated energy by human walking is stored in the two capacitors. By measuring the capacitor voltage V , we can calculate the amount of generated energy from different PEHs and subjects using $E = \frac{1}{2}CV^2$, where C is the capacitance.

Figure 15 presents the capacitor voltage of one subject, in which each *stair* corresponds to one gait cycle. The *stair* suggests that the energy is only produced within a small time slot, where the capacitor voltage climbs sharply, during each gait cycle. The stair-like capacitor voltage can be utilized for step counting as well [35]. The distribution of the average generated energy per step of the 20 subjects from the two PEHs is shown in Figure 16. It is apparent that the total amount of the harvested energy varies with different people (due to weight and walking style) ranging from

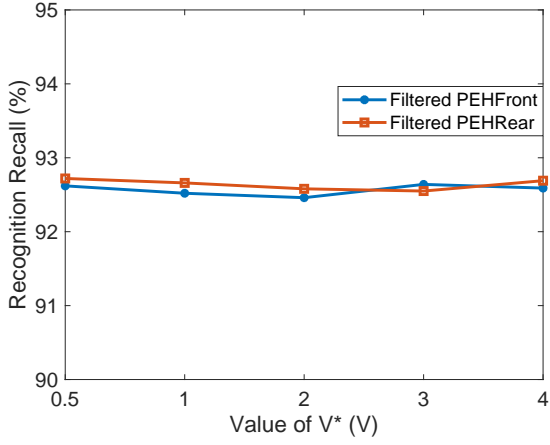
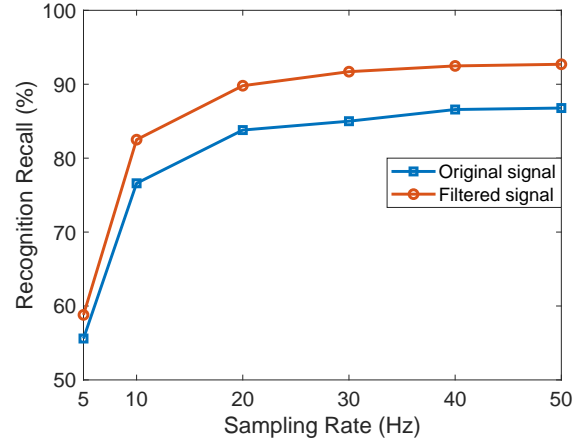
Fig. 12: Recall vs. Value of V^* .

Fig. 13: Recall vs. Sampling rate.

TABLE 1: Recognition performance vs. classifiers.

Classifier	Original signals				Filtered signals			
	PEHFront		PEHRear		PEHFront		PEHRear	
	Precision	Recall	Precision	Recall	Precision	Recall	Precision	Recall
KNN	55.43 (± 0.64)%	54.77 (± 0.47)%	51.87 (± 0.38)%	50.99 (± 0.35)%	63.75 (± 0.55)%	62.89 (± 0.60)%	62.03 (± 0.45)%	60.54 (± 0.50)%
SVM	67.82 (± 0.73)%	66.76 (± 0.68)%	66.68 (± 0.63)%	65.79 (± 0.65)%	71.47 (± 0.26)%	74.28 (± 0.29)%	73.85 (± 0.53)%	72.90 (± 0.48)%
SRC	77.19 (± 0.47)%	76.56 (± 0.51)%	76.57 (± 0.52)%	76.18 (± 0.57)%	85.86 (± 0.62)%	85.42 (± 0.58)%	87.02 (± 0.39)%	86.67 (± 0.42)%
ConvLSTM	85.26 (± 0.53)%	84.87 (± 0.55)%	84.56 (± 0.55)%	83.95 (± 0.62)%	90.85 (± 0.26)%	90.57 (± 0.25)%	91.63 (± 0.18)%	91.46 (± 0.27)%
UniLSTM	86.87 (± 0.54)%	86.50 (± 0.58)%	85.62 (± 0.43)%	85.30 (± 0.44)%	91.63 (± 0.33)%	91.50 (± 0.35)%	92.51 (± 0.35)%	92.41 (± 0.36)%
BiLSTM	96.79 (± 0.37)%	96.77 (± 0.38)%	96.98 (± 0.59)%	96.89 (± 0.59)%	98.41 (± 0.49)%	98.36 (± 0.51)%	98.95 (± 0.40)%	98.94 (± 0.41)%

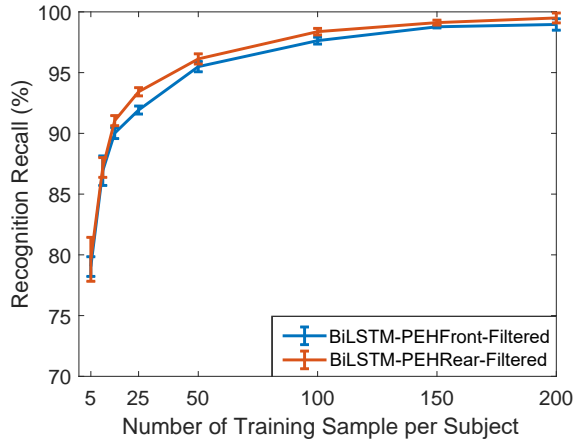


Fig. 14: Recall vs. Training size.

$109\mu J/\text{step}$ to $269\mu J/\text{step}$ with an average of $164\mu J/\text{step}$ ($92\mu J$ for PEHFront and $72\mu J$ for PEHRear). Assume that people walk in 2Hz, i.e., one gait cycle each second, a power output of $164\mu W$ can be achieved by wearing the insole in one foot, which is much more than the previous work [11] with only $1\mu W$ power by harvesting energy from walking-induced vibrations. More practically, such power generation is encouraging to extend the battery lifetime or even replace the battery for wearable devices.

Due to the realization of simultaneous energy harvesting and sensing, the proposed architecture can increase the

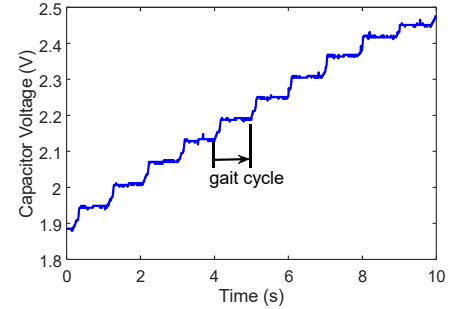


Fig. 15: Capacitor voltage during walking.

amount of harvested energy as well. Specifically, when two PEHs are mounted on the insole, SEHS can harvest energy with both PEHs (i.e., $72 + 92 = 164\mu J$) while the separated PEH architecture [6] has to choose one PEH for sensing and the other for energy harvesting. Around 78% ² more energy can be harvested in SHES if the front PEH is selected for energy harvesting and the improvement further lifts to 127% ³ when using the rear PEH for energy harvesting.

4.6 Power Consumption Measurements

To this end, we have demonstrated the superior performance of the proposed SEHS architecture in terms of both context detection and energy harvesting. However, the filter

1. $(164 - 92)/92 = 78\%$.
2. $(164 - 92)/92 = 78\%$.
3. $(164 - 72)/72 = 127\%$.

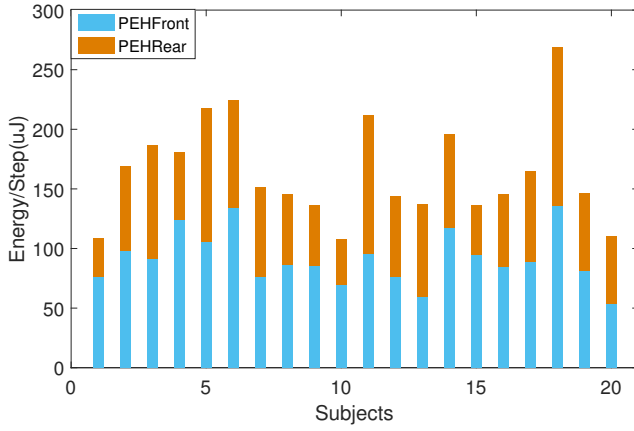


Fig. 16: The amount of energy generated per step from the two PEHs. The average generated energy of *PEHFront*, *PEHRear* and total is around $92\mu J$, $72\mu J$ and $164\mu J$ respectively.

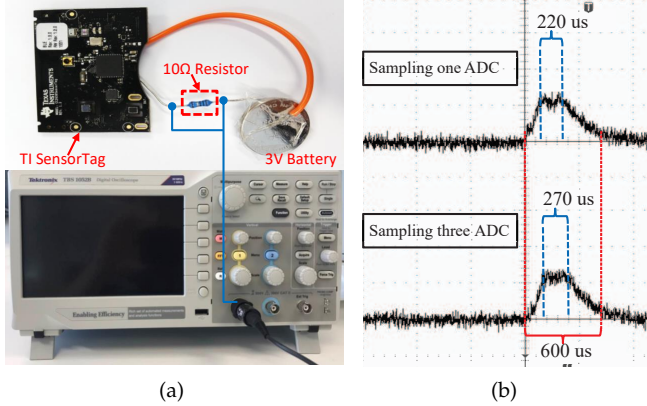


Fig. 17: (a) Measurement setup, (b) Profiling of ADC sampling.

in our prototype requires the capacitor voltage samples as an input, which is not used in the previous architectures [6], [11], [13]. Consequently, the power consumption overhead of sampling the capacitor voltage should be measured to assess the practicability of the filter. In fact, for each PEH, the proposed SEHS architecture uses a total of three ADCs (two for AC voltage and one for capacitor voltage), while previous method [6] uses only one ADC channel but with an amplifier consuming around $500\mu W$ power. Thus, we compare the overall sensing power consumption by measuring the power consumption of sampling ADCs.

4.6.1 Measurement setup

Figure 17(a) shows the experiment setup. We select the Texas Instrument SensorTag as the target device, which is equipped with an ultra-low power ARM Cortex-M3 MCU and 12-bits ADC. The SensorTag is running with the Contiki 3.0 operating system and programs that periodically sample one and three ADC channels are loaded. By connecting a 10Ω resistor between the SensorTag and a 3V coin battery, we measure the voltage on the resistor using a Tektronix TBS-1052B digital oscilloscope thereby deriving the current draw by using the voltage divided by 10Ω .

TABLE 2: Power consumption analysis when sampling at 40 Hz.

Event	[6] (One ADC)	SEHS (Three ADC)
MCU On Time (μs)	220	270
Total Event Time (μs)	600	600
MCU Sleep Power (μW)	6	6
ADC Power (μW)	482	511
Energy/Event (μJ)	0.29	0.31
Amplifier Power (μW)	500	0
Overall Power (μW)	29.43	18.12

4.6.2 Power consumption analysis

Figure 17(b) illustrates the profiling of an ADC sampling event. At the beginning, the MCU is configured to deep sleep mode, which consumes around $6\mu W$. Once the ADC sampling event is triggered, MCU wakes up and reads the value from ADC channels and then goes back to deep sleep mode. We can observe that the total time (refers to Total Event Time in Table2) of sampling one ADC channel and three ADC channels are almost equal at $600\mu s$ (marked with red dashed line), while the major difference comes from the time duration (refers to MCU On Time) that the MCU is turned on (marked with blue dashed line). Note that the process of MCU turning on/off requires time, which refers to the climbing and dropping stage in the profiling. As shown in the figure, the MCU On Time is $220\mu s$ and $270\mu s$ when sampling one and three ADC channels respectively. We calculate the average power consumption (refers to ADC Power) during the total event time with the built-in function of the oscilloscope and the results are $482\mu W$ and $511\mu W$ for one ADC and three ADC respectively.

Given a sampling rate of 40 Hz with duty-cycling, Table 2 presents a detailed power consumption analysis comparing previous architecture [6] (one ADC + amplifier) and the proposed SEHS architecture (three ADCs). First, we can see that sampling three ADC channels indeed incurs higher ADC Power but the increment is not much. We calculate the consumed energy for each sampling event and find that only $0.02\mu J$ additional energy is incurred, which suggests that the energy overhead of the proposed filter is subtle. Second, at 40 Hz sampling rate, we calculate the overall sensing power consumption when considering other components (e.g., amplifier) and MCU sleep time. Previous architecture consumes $29.43\mu W^4$ while our SEHS architecture only consumes $18.12\mu W^5$, achieve a power reduction of 38%. These results suggest that SEHS not only achieves better system performance in terms of energy harvesting and sensing, but also decreases the sensing power consumption compared to the state-of-the-art.

4. $P_{[6]} = (E_{ADC} + E_{Amp} + E_{Sleep})/t = (482 \times 600 \times 10^{-6} \times 40 + 500 \times 600 \times 10^{-6} \times 40 + 6 \times (1 - 600 \times 40 \times 10^{-6}))/1 = 29.43\mu W$.
5. $P_{SEHS} = (E_{ADC} + E_{Sleep})/t = (511 \times 600 \times 10^{-6} \times 40 + 6 \times (1 - 600 \times 40 \times 10^{-6}))/1 = 18.12\mu W$.

5 DISCUSSION

In this section, we discuss the limitations of current work and propose some potential solutions. First, the collected gait dataset came from volunteers walking only on soft ground (carpet) with normal speed. Prior investigations indicate that human gaits can be recognized with better accuracy for normal and fast walks compared to the case when the subject walks slowly [36], and hard walking ground enables higher accuracy than soft ground like grass [37]. Thus, a future work would be to collect SEHS data under more diverse walking grounds and speeds to assess the performance of SEHS more comprehensively. Second, energy harvesting from foot strikes is promising due to its high energy density [9], but the current work did not optimize energy harvesting efficiency. Techniques, such as maximum-power-point-tracking (MPPT) [38] could be used to maximize power extraction in shoe-based SEHS. Utilization of more advanced piezoelectric materials is another potential way to enhance energy generation [7]. Third, the number of subjects in our experiment is limited. It is expected that accurate gait detection will be more challenging when more subjects are involved. As a result, it may be necessary to explore more sophisticated deep learning models for SEHS-based gait recognition.

6 RELATED WORK

Our work relates to three main literature: context sensing using the output of PEH, recognition of human gait, and simultaneous energy harvesting and information sensing. We review these literature in this section.

6.1 PEH based Context Sensing

PEH possesses a well-known phenomenon called piezoelectric effect: when subjected to an external force, a PEH device generates AC voltage of which amplitude is positively correlated to the intensity of force. With appropriate signal processing and pattern recognition algorithms, the PEH signal can be used as a proxy to sense and detect motion-related context. Based on that, researchers have demonstrated a wide range of context sensing applications using PEH. Han et al. [39] built a shoe prototype with a PEH embedded. By analysing the generated AC waveforms, six different activities can be classified with over 90% accuracy. Lan et al. [13] designed a wearable PEH prototype to measure the vibrations when taking different transportation facilities (e.g., car, bus, train, and ferry), which achieved around 85% detection accuracy with typical machine learning. Other PEH based sensing applications include calorie expenditure estimation [40], gait recognition [11], [41], acoustic communication [8], [42], and so on.

Compared to conventional motion sensor based approaches, PEH based method significantly reduces the sensing power consumption as PEH is a completely passive element [9]. However, unlike specialized sensors that are fine-tuned for accurate measurements of the physical phenomenon, PEH can be only regarded as a crude sensing device. As a result, the context detection performance is inferior to specialized sensors.

Unlike existing works that only consider the sensing capability of PEH, our work takes its original functionality (energy harvesting) into consideration as well. We have

achieved simultaneous dual-use of a PEH and addressed the accompanying issues with signal processing. In addition, we introduce deep learning based classifiers to combat the low sensing capability of PEH.

6.2 Human Gait Recognition

Gait, the manner of human walking, has been recognized as a unique biometric feature of human. Recognizing human gait promises a number of applications such as people identification, device authentication, as well as health-related diagnostics like the Parkinson's disease [43]. Researchers have employed various modalities to capture human gait. The vision-based method utilizes camera sensors to capture visual images of human body and extracts the temporal transition features of a specific body part (e.g., joints) within a gait cycle [44]. The wireless-based method usually exploits RF signals (e.g., Wi-Fi [45], Radar [46]) or acoustic signal [47] to extract a user's gait. The underlying rationale is that walking style of users leaves unique signature on the wireless signals. Unlike the above methods that require deployment of gait capturing facilities in the space, wearable-based gait recognition method entails users to wear a motion sensor (like accelerometer and gyroscope) so that the gait can be reflected on the pattern of motion signals.

These methods have been proposed for a while and recent research focuses on the improvement of the recognition performance under more practical scenarios. Specifically, various deep neural networks have demonstrated their effectiveness in improving the recognition accuracy and robustness. For image data, Battistone et al. [48] proposed a graph based neural network (named Time based Graph Long Short-Term Memory, TGLSTM) to learn the long short-term dependencies of gait among frames. Chao et al. [49] integrated the set perspective into a convolutional neural network to improve the robustness under diverse viewing angles or different clothes. For inertial sensor gait data, Zou et al. [50] combined a convolutional neural network and a recurrent neural network to extract space and time domain features, which achieves 93% accuracy among 118 subjects.

Although the feasibility of using PEH for human gait recognition has been demonstrated by Xu et al. [11], our work differs in two aspects. First, instead of considering the sensing capability of PEH only, we proposed the simultaneous dual-use of PEH, identified the distortion effect of energy storage, and proposed a filter to resolve the effect. Second, Xu et al. exploits the hand-held PEH to capture vibrations during walking, while we utilized the foot-mounted PEH to capture the pressure of foot strikes. Our method is truly unobtrusive, unsusceptible to irregular hand motions, and can harvest more energy. Compared to the conference version of this work [51], we improved the gait recognition performance with deep learning.

6.3 Simultaneous Energy Harvesting and Information Sensing

With the sensing capability of energy harvesters being demonstrated, simultaneous energy harvesting and information sensing has attracted growing attention recently. For kinetic-based energy harvesting, instead of using additional ADC channels to minimize the impact of energy storage, Sandhu et al. [52] proposed the use of a DC-DC boost

converter to decouple the energy storage component from the transducer. However, the performance of this approach was not evaluated. For solar energy harvesting, Li et al. [53] proposed a self-powered gesture recognition system using arrays of photodiodes. The photodiodes operate in photo-voltaic mode to harvest energy from ambient light and their outputs are sampled to recognize different hand gestures.

In addition, the concept of SEHS is quite similar to simultaneous wireless information and power transfer (SWIPT) in wireless energy harvesting networks, where the RF signals are used for energy delivery as well as for information transmission. SWIPT has been extensively researched in the literature, including the typical structure [54], resource allocation strategy [55], and energy-information trade-off [56], which have been surveyed in [57]. Most recently, researchers mainly focus on the application of SWIPT in advanced mobile networks, such as 5G networks where the use of millimetre wave brings new challenges [58], [59], or unmanned aerial vehicle (UAV) networks where the mobility of UAVs affects the link quality dynamically [60], [61].

7 CONCLUSION

We have proposed SEHS, a novel architecture for simultaneous energy harvesting and gait recognition using the same piece of PEH hardware. To achieve high-accurate gait recognition, we proposed a filtering algorithm to minimize the sensing signal distortions caused by energy storage, and LSTM-based classifiers to mine useful information from noisy PEH data. We developed an insole-based prototype of SEHS and collected data from 20 subjects. Based on the experimental results, we have demonstrated that the SEHS prototype can harvest up to 127% more energy and detect human gait with 12% higher accuracy compared to the state-of-the-art. A power measurement confirms that SEHS achieves these performance improvements while actually consuming less power.

REFERENCES

- [1] S. Sudevalayam and P. Kulkarni, "Energy harvesting sensor nodes: Survey and implications," *IEEE Communications Surveys & Tutorials*, vol. 13, no. 3, pp. 443–461, 2011.
- [2] R. J. Vullers, R. Van Schaijk, H. J. Visser, J. Penders, and C. Van Hoof, "Energy harvesting for autonomous wireless sensor networks," *IEEE Solid-State Circuits Magazine*, vol. 2, no. 2, pp. 29–38, 2010.
- [3] "Bionic Power," <https://www.bionic-power.com/>, Online (accessed on June 30, 2020).
- [4] "Sole Power," <http://www.solepowertech.com/>, Online (accessed on June 30, 2020).
- [5] "MIDE Technology," <https://www.mide.com/>, Online (accessed on June 30, 2020).
- [6] T. Xiang, Z. Chi, F. Li, J. Luo, L. Tang, L. Zhao, and Y. Yang, "Powering indoor sensing with airflows: a trinity of energy harvesting, synchronous duty-cycling, and sensing," in *Proceedings of the ACM Conference on Embedded Networked Sensor Systems*, 2013, p. 16.
- [7] M. Hassan, W. Hu, G. Lan, A. Seneviratne, S. Khalifa, and S. K. Das, "Kinetic-powered health wearables: Challenges and opportunities," *Computer*, vol. 51, no. 9, pp. 64–74, 2018.
- [8] G. Lan, W. Xu, S. Khalifa, M. Hassan, and W. Hu, "VEH-COM: Demodulating vibration energy harvesting for short range communication," in *Proceedings of IEEE International Conference on Pervasive Computing and Communications*, 2017, pp. 170–179.
- [9] D. Ma, G. Lan, M. Hassan, W. Hu, and S. K. Das, "Sensing, computing, and communications for energy harvesting IoTs: A survey," *IEEE Communications Surveys & Tutorials*, vol. 22, no. 2, pp. 1222–1250, 2019.
- [10] D. Gafurov, "A survey of biometric gait recognition: Approaches, security and challenges," in *Proceedings of the Annual Norwegian Computer Science Conference*, 2007, pp. 19–21.
- [11] W. Xu, G. Lan, Q. Lin, S. Khalifa, M. Hassan, N. Bergmann, and W. Hu, "KEH-Gait: Using kinetic energy harvesting for gait-based user authentication systems," *IEEE Transactions on Mobile Computing*, vol. 18, no. 1, pp. 139–152, 2018.
- [12] H. Kalantarian, N. Alshurafa, T. Le, and M. Sarrafzadeh, "Monitoring eating habits using a piezoelectric sensor-based necklace," *Computers in biology and medicine*, vol. 58, pp. 46–55, 2015.
- [13] G. Lan, W. Xu, D. Ma, S. Khalifa, M. Hassan, and W. Hu, "Entrans: Leveraging kinetic energy harvesting signal for transportation mode detection," *IEEE Transactions on Intelligent Transportation Systems*, vol. 21, no. 7, pp. 2816–2827, 2020.
- [14] G. Poulin, E. Sarraute, and F. Costa, "Generation of electrical energy for portable devices: Comparative study of an electromagnetic and a piezoelectric system," *Sensors and Actuators A: physical*, vol. 116, no. 3, pp. 461–471, 2004.
- [15] C. Bowen, H. Kim, P. Weaver, and S. Dunn, "Piezoelectric and ferroelectric materials and structures for energy harvesting applications," *Energy & Environmental Science*, vol. 7, no. 1, pp. 25–44, 2014.
- [16] W. Xu, C. Javali, G. Revadigar, C. Luo, N. Bergmann, and W. Hu, "Gait-Key: A gait-based shared secret key generation protocol for wearable devices," *ACM Transactions on Sensor Networks*, vol. 13, 2017.
- [17] H. Zhong, Z. Xu, X. Zou, Y. Zou, L. Yang, and Z. Chao, "Current characteristic of high voltage capacitor charging power supply using a series resonant topology," in *Proceedings of the IEEE Industrial Electronics Society Annual Conference*, vol. 1, 2003, pp. 373–377.
- [18] Q. Huang, Y. Mei, W. Wang, and Q. Zhang, "Battery-free sensing platform for wearable devices: The synergy between two feet," in *Proceedings of the Annual IEEE International Conference on Computer Communications*, 2016, pp. 1–9.
- [19] H. A. Sodano, G. Park, and D. Inman, "Estimation of electric charge output for piezoelectric energy harvesting," *Strain*, vol. 40, no. 2, pp. 49–58, 2004.
- [20] S. J. Shultz, P. A. Houglum, and D. H. Perrin, *Examination of musculoskeletal injuries*. Human Kinetics, 2015.
- [21] S. Hochreiter and J. Schmidhuber, "Long Short-term Memory," *Neural computation*, vol. 9, no. 8, pp. 1735–1780, 1997.
- [22] H. Truong, S. Zhang, U. Muncuk, P. Nguyen, N. Bui, A. Nguyen, Q. Lv, K. Chowdhury, T. Dinh, and T. Vu, "CapBand: Battery-free successive capacitance sensing wristband for hand gesture recognition," in *Proceedings of the ACM Conference on Embedded Networked Sensor Systems*, 2018, pp. 54–67.
- [23] X. Zhang, L. Yao, S. Zhang, S. Kanhere, M. Sheng, and Y. Liu, "Internet of things meets brain-computer interface: A unified deep learning framework for enabling human-thing cognitive interactivity," *IEEE Internet of Things Journal*, vol. 6, no. 2, pp. 2084–2092, 2018.
- [24] T. Plötz and Y. Guan, "Deep learning for human activity recognition in mobile computing," *Computer*, vol. 51, no. 5, pp. 50–59, 2018.
- [25] "Understanding LSTM Networks," <http://colah.github.io/posts/2015-08-Understanding-LSTMs/>, 2015, Online (accessed on June 30, 2020).
- [26] A. Graves and J. Schmidhuber, "Framewise phoneme classification with bidirectional LSTM and other neural network architectures," *Neural networks*, vol. 18, no. 5-6, pp. 602–610, 2005.
- [27] S. Xingjian, Z. Chen, H. Wang, D.-Y. Yeung, W.-K. Wong, and W.-c. Woo, "Convolutional LSTM network: A machine learning approach for precipitation nowcasting," in *Proceedings of Advances in Neural Information Processing Systems*, 2015, pp. 802–810.
- [28] "Piezo system," <https://www.piezo.com/>, Online (accessed on June 30, 2020).
- [29] "Arduino 101," <https://www.arduino.cc/>, Online (accessed on June 30, 2020).
- [30] L. Prechelt, "Automatic early stopping using cross validation: quantifying the criteria," *Neural Networks*, vol. 11, no. 4, pp. 761–767, 1998.
- [31] K. Huang and S. Aiviyente, "Sparse representation for signal classification," in *Proceedings of Advances in Neural Information Processing Systems*, 2007, pp. 609–616.
- [32] S. Khalifa, G. Lan, M. Hassan, A. Seneviratne, and S. K. Das, "HARKE: Human activity recognition from kinetic energy har-

- vesting data in wearable devices," *IEEE Transactions on Mobile Computing*, vol. 17, no. 6, pp. 1353–1368, 2018.
- [33] D. J. Berndt and J. Clifford, "Using dynamic time warping to find patterns in time series," in *KDD workshop*, vol. 10, no. 16. Seattle, WA, 1994, pp. 359–370.
- [34] J. Benesty, J. Chen, Y. Huang, and I. Cohen, "Pearson correlation coefficient," in *Noise reduction in speech processing*. Springer, 2009, pp. 1–4.
- [35] G. Lan, D. Ma, W. Xu, M. Hassan, and W. Hu, "Capsense: Capacitor-based activity sensing for kinetic energy harvesting powered wearable devices," in *Proceedings of the 14th EAI International Conference on Mobile and Ubiquitous Systems: Computing, Networking and Services*, 2017, pp. 106–115.
- [36] M. Muaaz and C. Nickel, "Influence of different walking speeds and surfaces on accelerometer-based biometric gait recognition," in *Proceedings of the IEEE International Conference on Telecommunications and Signal Processing*, 2012, pp. 508–512.
- [37] S. Enokida, R. Shimomoto, T. Wada, and T. Ejima, "A predictive model for gait recognition," in *Proceedings of the IEEE Biometrics Symposium*, 2006, pp. 1–6.
- [38] B. Subudhi and R. Pradhan, "A comparative study on maximum power point tracking techniques for photovoltaic power systems," *IEEE transactions on Sustainable Energy*, vol. 4, no. 1, pp. 89–98, 2012.
- [39] Y. Han, Y. Cao, J. Zhao, Y. Yin, L. Ye, X. Wang, and Z. You, "A self-powered insole for human motion recognition," *Sensors*, vol. 16, no. 9, p. 1502, 2016.
- [40] G. Lan, S. Khalifa, M. Hassan, and W. Hu, "Estimating calorie expenditure from output voltage of piezoelectric energy harvester: an experimental feasibility study," in *Proceedings of the EAI International Conference on Body Area Networks*, 2015, pp. 179–185.
- [41] Q. Lin, W. Xu, G. Lan, Y. Cui, H. Jia, W. Hu, M. Hassan, and A. Seneviratne, "KEHKey: Kinetic energy harvester-based authentication and key generation for body area network," *Proceedings of the ACM on Interactive, Mobile, Wearable and Ubiquitous Technologies*, vol. 4, no. 1, pp. 1–26, 2020.
- [42] G. Lan, D. Ma, M. Hassan, and W. Hu, "HiddenCode: Hidden acoustic signal capture with vibration energy harvesting," in *Proceedings of IEEE International Conference on Pervasive Computing and Communications*, 2018, pp. 1–10.
- [43] A. Mirelman, P. Bonato, R. Camicioli, T. D. Ellis, N. Giladi, J. L. Hamilton, C. J. Hass, J. M. Hausdorff, E. Pelosin, and Q. J. Almeida, "Gait impairments in parkinson's disease," *The Lancet Neurology*, vol. 18, no. 7, pp. 697–708, 2019.
- [44] G. Zhao, G. Liu, H. Li, and M. Pietikainen, "3D gait recognition using multiple cameras," in *Proceedings of the IEEE International Conference on Automatic Face and Gesture Recognition*, 2006, pp. 529–534.
- [45] J. Zhang, B. Wei, W. Hu, and S. S. Kanhere, "WiFi-ID: Human identification using wifi signal," in *Proceedings of the IEEE International Conference on Distributed Computing in Sensor Systems*, 2016, pp. 75–82.
- [46] D. Tahmoush and J. Silvius, "Radar micro-doppler for long range front-view gait recognition," in *Proceedings of the IEEE International Conference on Biometrics: Theory, Applications, and Systems*, 2009, pp. 1–6.
- [47] W. Xu, Z. Yu, Z. Wang, B. Guo, and Q. Han, "AcousticID: Gait-based human identification using acoustic signal," *Proceedings of the ACM on Interactive, Mobile, Wearable and Ubiquitous Technologies*, vol. 3, no. 3, p. 115, 2019.
- [48] F. Battistone and A. Petrosino, "TGLSTM: A time based graph deep learning approach to gait recognition," *Pattern Recognition Letters*, vol. 126, pp. 132–138, 2019.
- [49] Q. Zou, Y. Wang, Q. Wang, Y. Zhao, and Q. Li, "Deep learning-based gait recognition using smartphones in the wild," *IEEE Transactions on Information Forensics and Security*, vol. 15, pp. 3197–3212, 2020.
- [50] H. Chao, Y. He, J. Zhang, and J. Feng, "Gaitset: Regarding gait as a set for cross-view gait recognition," in *Proceedings of the AAAI Conference on Artificial Intelligence*, vol. 33, 2019, pp. 8126–8133.
- [51] D. Ma, G. Lan, W. Xu, M. Hassan, and W. Hu, "SEHS: Simultaneous energy harvesting and sensing using piezoelectric energy harvester," in *Proceedings of the IEEE/ACM Third International Conference on Internet-of-Things Design and Implementation*, 2018, pp. 201–212.
- [52] M. M. Sandhu, "Phd forum abstract: Energy harvesting based sensing for the batteryless iot," in *2020 19th ACM/IEEE International Conference on Information Processing in Sensor Networks (IPSN)*. IEEE, 2020, pp. 373–374.
- [53] Y. Li, T. Li, R. A. Patel, X.-D. Yang, and X. Zhou, "Self-powered gesture recognition with ambient light," in *Proceedings of the 31st Annual ACM Symposium on User Interface Software and Technology*, 2018, pp. 595–608.
- [54] R. Zhang and C. K. Ho, "Mimo broadcasting for simultaneous wireless information and power transfer," *IEEE Transactions on Wireless Communications*, vol. 12, no. 5, pp. 1989–2001, 2013.
- [55] X. Lu, P. Wang, D. Niyato, D. I. Kim, and Z. Han, "Wireless networks with RF energy harvesting: A contemporary survey," *IEEE Communications Surveys & Tutorials*, vol. 17, no. 2, pp. 757–789, 2014.
- [56] Q. Shi, L. Liu, W. Xu, and R. Zhang, "Joint transmit beamforming and receive power splitting for miso swipt systems," *IEEE Transactions on Wireless Communications*, vol. 13, no. 6, pp. 3269–3280, 2014.
- [57] X. Lu, P. Wang, D. Niyato, D. I. Kim, and Z. Han, "Wireless networks with rf energy harvesting: A contemporary survey," *IEEE Communications Surveys & Tutorials*, vol. 17, no. 2, pp. 757–789, 2015.
- [58] Y. Liang, Y. He, J. Qiao, and A. P. Hu, "Simultaneous wireless information and power transfer in 5g mobile networks: A survey," in *2019 Computing, Communications and IoT Applications (ComComAp)*. IEEE, 2019, pp. 460–465.
- [59] A. Rajaram, R. Khan, S. Tharranetharan, D. N. K. Jayakody, R. Dinis, and S. Panic, "Novel swipt schemes for 5g wireless networks," *Sensors*, vol. 19, no. 5, p. 1169, 2019.
- [60] X. Hong, P. Liu, F. Zhou, S. Guo, and Z. Chu, "Resource allocation for secure uav-assisted swipt systems," *IEEE Access*, vol. 7, pp. 24 248–24 257, 2019.
- [61] W. Wang, J. Tang, N. Zhao, X. Liu, X. Y. Zhang, Y. Chen, and Y. Qian, "Joint precoding optimization for secure swipt in uav-aided noma networks," *IEEE Transactions on Communications*, 2020.



Dong Ma is a Ph.D. student in the School of Computer Science and Engineering, the University of New South Wales, Sydney, Australia. He received the B.S. degree in communication engineering from Central South University, China, in 2014. His research interests include Internet of Things, Pervasive Computing, Visible Light Sensing, and Energy Harvesting. He is a student member of the IEEE.



Guohao Lan is currently a Postdoctoral Research Associate with the Department of Electrical and Computer Engineering, Duke University, Durham, NC 27708, USA. Prior to this, he obtained his Ph.D. degree in Computer Science and Engineering from the University of New South Wales, Australia. He received the M.S. degree in Computer Science from Korea Advanced Institute of Science and Technology (KAIST), Korea, in 2015, and the B.E. degree in Software Engineering from Harbin Institute of Technology, China, in 2012. His research interests include wireless sensor networks, and mobile computing systems. He is a member of the IEEE.



Weitao Xu is currently a Research Associate at the College of Computer Science and Software Engineering, Shenzhen University, China. He received his Ph.D. degree from the University of Queensland in 2017. He received the bachelor of engineering and the master of engineering degrees in 2010 and 2013, respectively, from the School of Information Science and Engineering, Shandong University, Shandong, China. He is a member of the IEEE.



Mahbub Hassan is a Full Professor in the School of Computer Science and Engineering, the University of New South Wales, Sydney, Australia. He is a Senior Member of IEEE and served as a Distinguished Lecturer of IEEE (COMSOC) for 2013-2016. He is currently an Editor of IEEE Communications Surveys and Tutorial and has previously served as Guest Editor for IEEE Network, IEEE Communications Magazine, IEEE Transactions on Multimedia, and Area Editor for Computer Communications. Professor Hassan has earned a PhD from Monash University, Australia, and an MSc from University of Victoria, Canada, both in Computer Science. More information about Professor Hassan is available from <http://www.cse.unsw.edu.au/~mahbub>.

Professor Hassan has earned a PhD from Monash University, Australia, and an MSc from University of Victoria, Canada, both in Computer Science. More information about Professor Hassan is available from <http://www.cse.unsw.edu.au/~mahbub>.



Wen Hu is an Associate Professor at School of Computer Science and Engineering, the University of New South Wales (UNSW). His research focuses on the novel applications, low-power communications, security and compressive sensing in sensor network systems and Internet of Things (IoT). Hu published regularly in the top rated sensor network and mobile computing venues such as ACM/IEEE IPSN, ACM SenSys, ACM transactions on Sensor Networks (TOSN), IEEE Transactions on Mobile Computing (TMC), Proceedings of the IEEE. Hu is a senior member of ACM and IEEE, an associate editor of ACM TOSN and the general chair of CPS-IoT Week 2020, as well as serves on the organising and program committees of networking conferences including ACM/IEEE IPSN, ACM SenSys, ACM MobiSys, ACM MobiCom, and IEEE ICDCS.